Article **Journal of Research and Development**
June 2023, Vol.9 No.23 17-28

Strain localization instability in seafloor spreading centers of the Carmen Basin, southern Gulf of California

Inestabilidad de la localización de la deformación en los centros de extensión del fondo marino de la Cuenca del Carmen, sur del Golfo de California

JULIÁ-MIRALLES, Marc†, YARBUH, Ismael*, SPELZ, Ronald M. and NEGRETE-ARANDA, Raquel

Universidad Autónoma de Baja California, Facultad de Ciencias Marinas, Departamento de Geología, Campus Ensenada, Baja California, México.

ID 1st Author: *Marc, Juliá-Miralles* / **ORC ID:** 0000-0001-8201-3566, **CVU CONAHCYT ID:** 1011828

ID 1st Co-author: *Ismael, Yarbuh* / **ORC ID:** 0000-0002-7146-3841, **CVU CONAHCYT ID:** 381344

ID 2nd Co-author: *Ronald M., Splez* / **ORC ID:** 0000-0002-9561-355X, **CVU CONAHCYT ID:** 37229

ID 3rd Co-author: *Rauqel, Negrete-Aranda* / **ORC ID:** 0000-0003-3049-4374, **CVU CONAHCYT ID:** No. 92968

DOI: 10.35429/JRD.2023.23.9.17.28 Received: January 20, 2023; Accepted: June 30, 2023

Abstract

This study provides new insights into the geological evolution of the Carmen Basin (CB) in the southern Gulf of California (GC). Using high-resolution bathymetry and seismic reflection profiles, we establish a plate-kinematic framework for this oblique-divergent rift system. By analyzing the crustal composition, we investigate the growth of the bounding transform faults and their role in accommodating transtensional shearing. We propose that the mantle upwelling beneath the CB is a northward extension of the East Pacific Rise. The CB consists of three sub-basins with distinct geometries, morphologies, and evolutionary histories. While the southern and central sub-basins are mostly abandoned, the northern sub-basin is currently experiencing seafloor spreading. This is supported by the presence of younger oceanic crust, approximately less than 1.5 Ma, juxtaposed with older oceanic crust that aligns in age with the nearby Guaymas and Farallon basins to the north and south, respectively. Our findings also indicate favorable geological conditions in the CB for the development of hydrothermal systems similar to those observed in the neighboring Guaymas and Pescadero basins in the southern GC.

Simple shear deformation, Crustal lithology, Fast seafloor spreading

Resumen

El presente trabajo proporciona nuevos conocimientos sobre la evolución geológica de la Cuenca de Carmen (CB) en el sur del Golfo de California (GC). A partir de datos de batimetría de alta resolución y perfiles sísmicos de reflexión, establecemos la cinemática de la tectónica de placas para este sistema de rift oblicuo-divergente. Al analizar la composición de la corteza, investigamos el crecimiento de las fallas transformes y el papel que juegan estas para acomodar la cizalla transtensional. Proponemos que el ascenso del manto por debajo de la CB es una extensión de la dorsal del Pacífico Oriental. La CB consta de tres sub-cuencas con geometrías, morfologías e historias evolutivas distintas. Mientras que las sub-cuencas del sur y del centro están prácticamente abandonadas, la sub-cuenca del norte está experimentando actualmente la expansión activa del fondo marino. Esto se apoya en la presencia de corteza oceánica más joven, aproximadamente menor que 1.5 Ma, asociada con una corteza oceánica más antigua que tiene la misma edad que las cuencas de Guaymas y Farallón que delimitan a la CB hacia el norte y sur, respectivamente. Nuestros resultados también indican condiciones geológicas favorables en la región para el desarrollo de sistemas hidrotermales similares a los observados en las cuencas vecinas de Guaymas y Pescadero en el sur del GC.

Deformación por cizalla simple, Litología de la corteza, Rápida dispersión del fondo marino

Citation: JULIÁ-MIRALLES, Marc, YARBUH, Ismael, SPELZ, Ronald M. and NEGRETE-ARANDA, Raquel. Strain localization instability in seafloor spreading centers of the Carmen Basin, southern Gulf of California. Journal of Research and Development. 2023. 9-23:17-28.

* Author's Correspondence (E-mail: uyarbuh@uabc.edu.mx)
† Researcher contributing as first author.

Introduction

The rifting dynamics of the Gulf of California (GC) still remain considerable gaps in information due to unexplored regions in the southern GC (Figure 1), where geological data has poor spatial and temporal resolution (Sutherland et al., 2012; Martín-Barajas et al., 2013; Macias-Iñiguez et al., 2019; Ramírez-Zerpa et al., 2022). The southwestern margin of the GC experiences active rifting, accompanied by east-directed low-angle normal faults and simple shear zones (Buck, 1988; Wernicke and Axen, 1988; Lavier et al., 1999; Fletcher and Spelz, 2009; Umhoefer et al., 2020; Figure 1). These structures accommodate significant crustal extension along the San Juan de Los Cabos and San Juan de Los Planes faults (Fletcher et al., 2000; Fletcher and Munguia, 2000; Bot et al., 2016), resulting in ~40 km of linear extension towards the continental-oceanic crust transition east of the Cerralvo basin, adjacent to the deep-water Pescadero basin complex (Figure 1; Macias-Iñiguez et al., 2019; Ramírez-Zerpa et al., 2022).

This study focuses on providing new insights into the structural evolution of the Carmen Basin (CB) from high-resolution bathymetry (Figure 2) and two-dimensional (2D) seismic reflection profiles (Figure 3-5). We characterize the geometry and structure of the CB to identify crustal deformation, basement lithology, seismic-stratigraphy, and magmatic events. Finally, we contrast our results with mantle tomography data (Wang et al., 2009; Di Luccio et al., 2014; Ferrari et al., 2018) to reconstruct the structural evolution of the CB, and discuss how the opening of the GC contributes to the formation of new oceanic crust, the deformation of the oceanic lithosphere to accommodate younger spreading centers, and the kinematics of the transform faults that constitute the modern Pacific and North America plate boundary.

Tectonic evolution of the Gulf of California

The northwestern continental margin of Mexico has undergone a significant transformation from a convergent plate boundary to an oblique-divergent margin (Balestrieri et al., 2017). During the Paleogene, the Farallon oceanic plate subducted beneath North America, creating a divergent plate boundary between the Farallon plate and the Pacific plate.

During the Eocene, the Farallon plate was largely consumed, and a portion of the East Pacific Rise approached the paleo-trench (Atwater, 1970; Stock and Hodges, 1989; Bunge and Grand, 2000; Wright et al., 2016). In the Oligocene, direct interaction occurred between the East Pacific Rise and the paleo-trench, and along the North American plate. The proximity of the Pacific-Farallon divergent margin to the continental borderland marked the transition from subduction to lithospheric extension and dextral shearing along the Magdalena plate boundary derived from the Farallon plate. Intraplate magmatism also occurred along the Baja Peninsula due to viscous shearing (Figure 1; Spencer and Normark, 1979; Atwater and Stock, 1998; Fletcher et al., 2007; Negrete-Aranda et al., 2013).

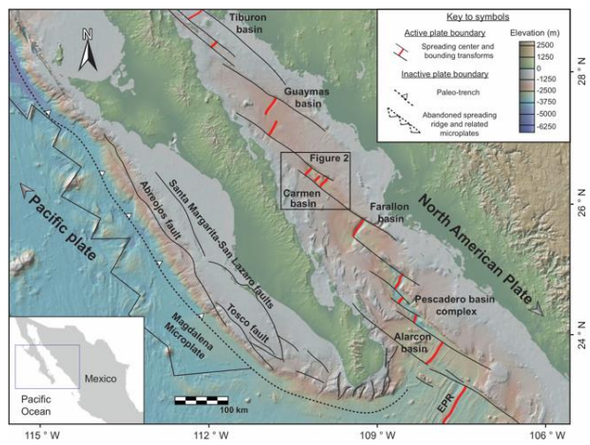

Figure 1 An overview of the tectonic features in the southern Gulf of California. It displays the plate motion (black arrows), the transform fault system (black lines), pull-apart basins, and spreading centers (red lines). The study area with the location of the Carmen Basin is denoted by the black box (Figure 2). Figure adapted from Julià-Miralles et al. (submitted). The abbreviation "EPR" is used for the East Pacific Rise. Base map sourced from GeoMapApp (http://www.geomapapp.org).

During the early Miocene, the Farallon plate fragmented into several smaller plates, with buoyant remnants of the Farallon plate and a section of the North American plate coupling with the Pacific Plate and moving northwestward (Nicholson et al., 1994; Bohannon and Parson, 1995). Dextral-oblique shearing migrated eastward from the continental margin into the current GC, leading to overall crustal thinning in the region (Stock and Hodges, 1989; Fletcher et al., 2007; Umhoefer et al., 2020).

ISSN-On line: 2444-4987

This process was accompanied by an increase in rift obliquity, facilitated by a change in plate motion direction, resulting in the localization of the plate boundary, marine incursion in the northern GC at ~8 Ma, and the formation of shallow water basins (Bennett et al., 2016; Umhoefer et al., 2018; Ramírez-Zerpa et al., 2022). The current tectonic regime was established ~6 Ma, when the East Pacific Rise extended into the mouth of the GC, separating the Baja California Peninsula from the North American continent (Wang et al., 2009, 2013; Lizarralde et al., 2007; Piñero-Lajas, 2008; Ramírez-Zerpa et al., 2022). Magma accretion was made possible by the propagation of right-lateral, right-stepping transform faults, which transferred motion oblique to the primary movement of the Baja California Microplate (Fletcher et al., 2007).

Methods

High-resolution bathymetry data was acquired for the CB basin during the FK210922 expedition in October 2021, conducted aboard the R/V Falkor and operated by the Schmidt Ocean Institute. The data was collected using an EM 302 multi-beam echo sounder, capturing 432 soundings per swath with dual swath mode for up to 864 soundings. The bathymetry data covered a depth of ~3,600 m and were gridded at 40-m intervals. The survey lines were spaced 5 km apart, running sub-parallel to the master transform faults that bound the basin.

Two dimensional (2D) seismic reflection data was used along ~65 km to constrain the rift evolution of CB. Data collected in 2006 aboard the R/V Francisco de Ulloa during a collaborative data collection campaign involving CICESE and Scripps Institution of Oceanography at UCSD. A three-stage workflow was applied to analyze the seismic data and generate sub-surface structural images. This workflow enabled frequency extraction, multiple mitigation, signal amplitude equalization, noise reduction, precise ray trajectory correction, spurious effect attenuation, and conversion from two-way travel time to depth (TWTT) to depth in meters (Yilmaz, 2001). Key structural features such as fault planes, folds, grabens, and sedimentary sequences were identified using well-proven criteria.

Quantitative parameters, such as fault length and dip, stratal thicknesses, subsidence, and sedimentary sequence boundaries, were also determined. Seismic facies analysis identified basement lithology and sedimentary material, including magmatic injections and geothermal fluids, in the form of mosaic patterns of highly reflective and low-reflectance surfaces (Chopra and Marfurt, 2007).

Results

Map view geometry of the Carmen Basin

The CB is a narrow, rhomboidal basin that has evolved from incipient to extremely mature basins. It is 80 km long and 20 km wide, with a length-to-width ratio of 4:1. Two sub-parallel, northwest-oriented principal displacement zones control the northeastern and southwestern margins of the CB. The Carmen transform fault extends 150 km, while the Farallon transform in the southwest stretches 200 km. These bounding zones overlap and connect through a traverse system of en-echelon oblique-extensional normal faults, creating three distinct sub-basins (Figure 2). The bathymetry of the CB reveals significant footwall uplift along the trace of the transform faults, which is accommodated by an array of en-echelon segmented basin sidewall faults developed on both flanks of the CB (Figure 2). Along these steep faults, gravitational instabilities develop, leading to rapid and episodic slumping and grain flows, forming distinct cliffs with landslide crowns and scarps along the basin's outer margin. However, the primary sediment routing system for infilling the CB appears to be a submarine dendritic drainage system originating from the tips of the principal displacement zones (Figure 2).

ISSN-On line: 2444-4987

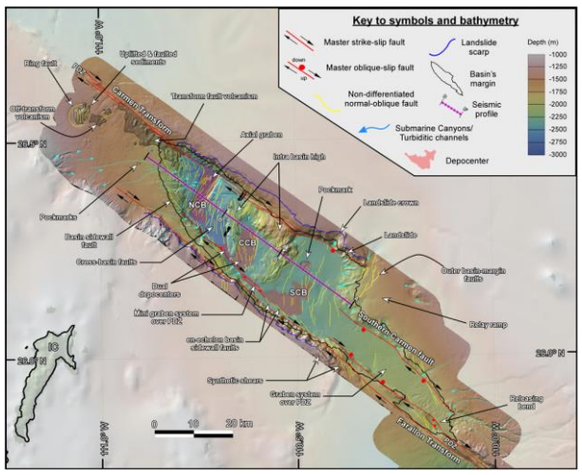

Figure 2 Structural map of the Carmen Basin (CB) illustrating its two-dimensional architecture and geometry. High-resolution (40-m) bathymetry is superimposed on faded GMRT bathymetry. Abbreviations: SCB = Southern Carmen Basin; CCB = Central Carmen Basin; NCB = Northern Carmen Basin. Figure adapted from Julià-Miralles et al. (submitted)

At a finer scale, Figure 2 reveals a cross-basin fault system that propagates obliquely to the principal displacement zones. This fault system originates a left-stepping arrangement of synthetic Riedel shear faults that curve into an elongated sigmoidal shape, connecting the sidewall faults at both sides of the basin. The resulting horst-graben structure divides the CB into three distinct sub-basins with contrasting morphologies, namely, the southern CB, the central CB, and the northern CB.

The southern CB features the shallowest depocenter (~2200 mbsl) among all the sub-basins, delimited by an array of cross-basin faults oriented at a high angle to the bounding transform faults (Figure 2). The northern margin is bounded by an uplifted and translated crustal block, while the southern margin is delimited by a strike-slip relay ramp that transfers and accommodates the deformation between the Carmen transform fault and a secondary oblique-slip fault called the "Southern Carmen fault." The relay ramp lies on the footwall of the oblique Southern Carmen fault, controlling a prominent graben system in the southeastern corner of the CB (Figure 2).

The central CB (~2400 mbsl) acts as a connection between the northern and southern CB. It is bordered by two intra-basin highs that have formed in response to a series of cross-basin faults that originate from synthetic Riedel shears along the basin's sidewalls (Figure 2).

These structural highs can be attributed to block translation and rotation during the early stages of basin development. The geometry of the central CB is elongated and oval, with a northern orientation, suggesting that deformation may have ceased in this region, allowing the modern northern CB spreading center to migrate further north (Figure 2). Variations in basin topography suggest the juxtaposition of different materials, with structural highs representing either a crystalline basement or indicating late Miocene-Pleistocene volcanic activity.

The northern CB represents the deepest part of the entire CB, reaching depths of ~2800 mbsl. The basin exhibits a broad nested graben where rocks have undergone downward displacement along an array of cross-basin faults connecting the bounding master faults (Figure 2). The overall geometry and geomorphological features of the northern CB suggest that the basin has evolved due to transtensional deformation, similar to the Pescadero basin complex located further south. The northern CB hosts the current seafloor spreading center, featuring a short and narrow axial graben oriented sub-perpendicular to the principal displacement zones (Figure 2). Magmatic activity is conspicuous not only across the spreading center but also along the bounding master faults and inside the sub-basins.

Crustal structure and stratigraphy of the Carmen Basin

The seismic interpretation of lines AA'-CC' (Figures 3-5) and morphology analysis reveal the structural evolution of the CB. The sub-basins exhibit two distinct seismic facies: high-energy successions and low-energy sequences. The first facies consists of rocks with prominent high-amplitude continuous reflectors, showing strong lateral coherence. This unit is likely composed of well-bedded pelagic sediments deposited in a low to medium-energy environment. The second facies consists of sedimentary rocks interbedded with and bounded by the distinct reflection of the first unit. Within the second rock unit, a diffuse seismic facies is observed, characterized by numerous short wavy reflections with poor lateral continuity, extending up to 1 km individually.

ISSN-On line: 2444-4987

These low-amplitude chaotic reflections represent higher energy accumulations of clastic sediments within the second seismic facies. The second facies appears dimmer than the first facies, giving the basin fill the appearance of thick accumulations of oceanic turbidites.

The seismic section also reveals a third facies characterized by a thick and homogeneous series of highly reflective, ropey-like layers with sigmoidal, semi-continuous reflection geometry and strong lateral coherence (Figures 3-5). These rocks exhibit more nonplanar reflections and limited lateral coherence, with individual reflections extending up to 1 km. The third unit spans a depth range from 2900 m at the depocenter of the actual axial graben to 1700 m in shallower sections (Julià-Miralles et al., submitted).

Profile AA' extends 28 km and images the southern CB, which trends NW-SE parallel to the axis of the CB (Figure 3). The profile shows a symmetrical horst-graben system delimited by two high-angle cross-basin faults, resulting in a topographic step of ~300 m in relief. The basin-bounding faults created sufficient subsidence to accommodate the deposition of ~550 m of syn-tectonic sedimentary sequences sourced from the continental shelf of the Baja California Peninsula and Sonora rifted margins. The most basal successions (~250 m-thick) have low-amplitude chaotic reflections, suggesting poor stratification and high-energy sedimentation (Figure 3). Growth strata sedimentation changes up-section to a seismic facies ~300 m-thick with good coherence and high-amplitude continuous reflections, suggesting low-medium energy sedimentation. The two seismic facies lie unconformably on the acoustic basement, interpreted as sigmoidal semi-continuous seismic reflections at 2800 m-depth on the southeastern flank of the symmetric graben and laterally terminate against the walls of an inactive nested fault system verging NW (Figure 3). The northwestern footwall block of the southern CB is interpreted to be a highly fractured oceanic basement, while the southeastern footwall block is covered by 300 m of sediments. The transition from horizontal sedimentation to a tilted configuration along a growing fault is interpreted to be the product of fault rotation, resembling negative flower structures Dooley and McClay, 1997; Wu et al., 2009; Julià-Miralles et al., submitted).

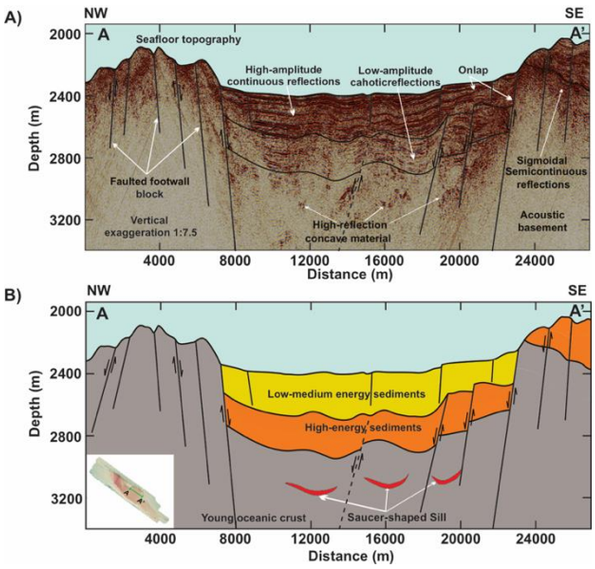

Figure 3 Seismic profile A-A' across the southern Carmen Basin (CB). A) Structural and stratigraphic seismic interpretation. B) Interpreted geologic cross-section. The seismic image reveals a wide, symmetrical graben bounded by two primary normal faults, identified as cross-basin structures (Figure 2). Panel (B) highlights high-amplitude reflections at ~3100 m depth, possibly indicating an ancient spreading center near abandoned nested normal faults. Figure adapted from Julià-Miralles et al. (submitted)

Profile BB' spans 20 km across the central CB (Figure 4), with high-amplitude curvy reflections indicating young oceanic crust. The central CB has an asymmetrical half-graben architecture, with a domino fault system defining the southern flank. The basal sedimentary package shows a pronounced tilt towards the SE, and the acoustic basement displays high-amplitude sigmoidal semi-continuous reflections at depths of 2800 m and 2400 m, suggesting an oceanic crust composed of volcanic flows. This material can be correlated with basement rocks in the southern CB, located further south of the CB. In the middle of the central CB (Figure 4), at a depth of 2700 mbsl, there is a 1 km-wide block of highly reflective material that stands above the well-defined basement to the NW. The seismic expression of this feature resembles the ropey textured reflections seen in the surrounding basement but appears brighter. It may indicate the axis of an extinct seafloor spreading system that was active prior to the deposition of the overlying sedimentary sequence (Figure 4). Above this feature and the surrounding oceanic basement, there is a syn-tectonic sedimentary package that reaches a thickness of ~300 m, showing seismic stratigraphy similar to the southern CB (Julià-Miralles et al., submitted).

ISSN-On line: 2444-4987

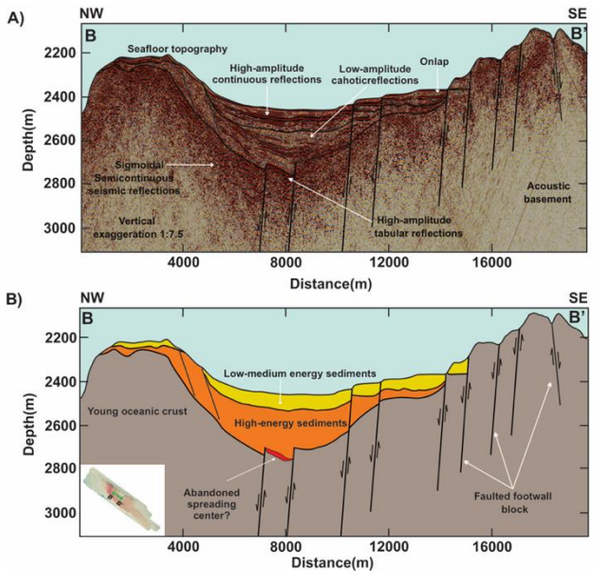

Figure 4 Seismic profile B-B' across the central Carmen Basin (CB). A) Structural and stratigraphic seismic interpretation. B) Interpreted geologic cross-section. The image reveals an asymmetrical half-graben structure NW-striking normal faults accommodating ~300 m of syn-tectonic sedimentation. In panel (B), at ~2750 m depth, tabular high-amplitude reflections suggest the presence of an ancient spreading center, similar to Figure 3. Figure adapted from Julià-Miralles et al. (submitted).

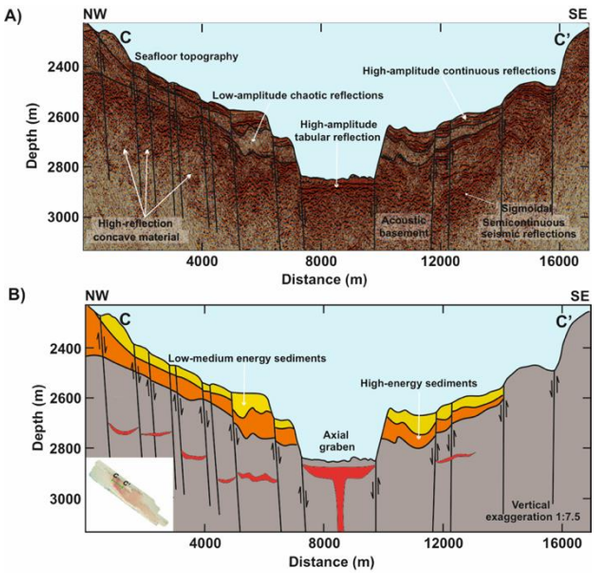

Figure 5 Seismic profile C-C' across the northern Carmen Basin (CB). A) Structural and stratigraphic seismic interpretation. B) Interpreted geologic cross-section. The profile intersects the axial graben of the northern CB. The spreading center is interpreted as asthenospheric mantle reaching the seafloor to generate new ocean crust. Figure adapted from Julià-Miralles et al. (submitted).

Profile CC' cuts through the northern CB with a length of 17 km, representing the deepest and narrowest sub-basin within the CB (Figure 5). The axial graben is bounded by inward-stepping normal faults striking perpendicular to the principal displacement zone. The sedimentary fill in the northern CB is notably thinner compared to other Carmen sub-basins, measuring only 200-300 m thick. The faults that define the margins of the innermost graben exhibit a throw of only 100 m, as indicated by the small steps observed on the top of the oceanic basement (Figure 5). The two seismic facies, characterized by high and low-amplitude reflection, are correlated on both flanks of the basin and are clearly dissected by the graben. On the southeastern flank of the axial graben, the sigmoidal semi-continuous reflections reach the seafloor topography at a depth of 2500 m, suggesting the young oceanic crust outcrops. On the northwestern flank of the axial graben, the oceanic basement is covered by the two sedimentary units interpreted throughout the CB. The inner graben represents the active spreading axis of the CB (Julià-Miralles et al., submitted; Figure 5).

Discussion

Crustal lithology and sill intrusion in the Carmen Basin

The CB acoustic basement is composed of highly reflective ropey layers with good lateral continuity, similar to those found in neighboring basins. These layers are identified as basaltic lava flows and intruded sills within sedimentary deposits (Piñero-Lajas, 2008; Lizarralde et al., 2007; Kluesner, 2011). The basement rocks outcrop widely along the three sub-basins of the CB, the spreading center, and the structural highs, forming approximately 80 km of newly formed oceanic crust. The Guaymas, Carmen, and Farallon basins are embedded in a slab of oceanic crust, with the eastern transition between continental and oceanic crust delimited by en-echelon scarps and the western and southwestern basin margins defined by rotated blocks along the Baja California continental shelf border (Macias-Iniguez et al., 2019). The CB separates the Guaymas and Farallon basins through an oceanic-oceanic crustal boundary, with the Carmen transform fault and Farallon transform fault bounding the CB being younger than the oceanic crust along the inner margins of the Guaymas and Farallon basins.

ISSN-On line: 2444-4987

The seismic profiles across the CB reveal concave, high-reflection material interpreted as saucer-shaped igneous sills, which are associated with overburden deformations, fluid migration through faults, and potential feeder networks (Negrete-Aranda, 2019, 2021; Sarkar et al., 2022; Julià-Miralles et al., submitted). These shallow sills are observed within a young oceanic crust, representing sites of magmatic crustal accretion in the actively growing basin. Off-axis intrusions into high-energy sediments are also identified between old oceanic crust and low-medium energy sediments.

Transform faults kinematics and crustal deformation in the Carmen basin

Mantle dynamics play a crucial role in the spreading rate of rift zones and core-complex accretion in mid-ocean ridge environments (Buck, 1993; Howell et al., 2019). Slow-spreading ridges exhibit buoyant mantle upwelling and focused melt migration beneath ridge centers, while fast-spreading ridges show uniform mantle upwelling along the ridge axis (Kuo and Forsyth, 1988; Lin et al., 1990; Escartin and Lin, 1995; Canales et al., 2000, 2003; Gregg et al., 2006, 2007). The formation of the CB in the southern GC is suggested to have occurred after seafloor spreading initiated in the Farallon and Guaymas basins. Kinematic instability of the bounding faults led to the propagation of the Carmen transform fault and Farallon transform fault, eventually forming the CB. The stability of this family of boundaries is influenced by the pooling of erupted lavas observed in topographic lows within the transform fault domain. This leaky magmatic accretion results from the presence of intermediate-fast-slipping transform faults, a configuration frequently observed at the East Pacific Rise (Gregg et al., 2007). The CB could be a result of an intra-transform spreading center system driven by fast rifting (Gregg et al., 2007; Gerya 2010; Julià-Miralles et al., submitted), where penetrative deformation along the main axis of the basin leads to different stages of deformation, resulting in the formation of sub-basins with contrasting geometries.

In the case of the CB, mantle upwelling and fast rifting were responsible for the formation of new oceanic spreading centers connected by intermediate-fast slipping transform faults (Wang et al., 2009; Zhao, 2004; Di Lluccio, 2014; Negrete-Aranda et al., 2021). The rapid formation of the CB (Umhoefer, 2011) may resolve the sequential abandonment of its sub-basins, with deformation progressing from the southeastern region of the CB towards the northwestern region, where the current active spreading center is located. Another hypothesis to explain the more youthful genesis of the CB is that the cross-basin faults do not fully propagate and instead become abandoned, leading to the development of new cross-basin faults toward the active zones connecting the bounding faults, namely the Carmen transform fault and Farallon transform fault. The significant extension rate in this part of the GC likely contributed to the abandonment of the southern and central CB sub-basins, leading to the formation of the northern CB where the current spreading center is actively accreting modern oceanic crust (Julià-Miralles et al., submitted).

The CB consists of three distinct overlapping spreading centers within the same plate-margin segment, indicating significant instability in the localization of the spreading process. These centers form grabens with increasingly advanced pull-apart geometries from south to north, suggesting strain migration in that direction. Lithospheric strength plays a crucial role in strain localization, and compositional and thermal heterogeneities in the upper mantle are likely to have significantly influenced the positioning of spreading axes. Seismic tomography conducted by Wang et al. (2009) and Di Luccio et al. (2014) revealed robust upwelling with low-shear velocity near the more stable Guaymas and Farallon spreading systems. However, these mantle anomalies are offset toward the east compared to the surface trace of these spreading systems. The distribution of applied tectonic loads along the plate margin is another factor that strongly controls strain localization.

ISSN-On line: 2444-4987

Fletcher et al. (2007) proposed that the capture of the Baja California microplate was driven by the coupling of the continental crust with the underplated oceanic lithosphere Farallon-derived microplates that became welded to the Pacific plate across the paleo East Pacific Rise west of Baja California. Therefore, tectonic loads should be most strongly applied to the lithosphere along the trailing edge of the shallowly underplated Farallon slab along the western limit of the Baja California microplate.

Conclusions

The seismic analysis of the CB reveals the acoustic basement consists of volcanic rocks, indicating the formation of a new oceanic floor within the basin. Multiple faults intersect the acoustic basement, contributing to penetrative deformation. The sedimentation process in the sub-basin system is dynamic and influenced by mass movements from sidewall fault scarps and dendritic drainage systems. These structures have accumulated significant amounts of detrital sediments.

The oceanic crust of the CB is delimited by major basin sidewall faults, alongside magmatic activity occurring along transform faults. This magmatic accretion suggests the presence of intermediate-fast-slipping transform faults, separated by a segment of intra-transform spreading center. This configuration resembles the extensional dynamics observed in the East Pacific Rise towards the mouth of the GC.

The formation of the CB initiated in the southern region, with sediment thickness gradually decreases towards the northern CB. The reactivation of the East Pacific Rise beneath the GC plays a significant role in influencing the relocation of spreading axes. Areas with thinner and fractured crust become favored during this process. As a result, sub-basins and fossil spreading centers are abandoned in the southern and central CB, while an active spreading center persists in the northern CB. Further north, near the Carmen transform fault, the development of ring faults and mud volcanoes may contribute to the future migration of a spreading center.

Acknowledgments

We thank the Schmidt Ocean Institute and the *R/V Falkor* crew for their support during expedition FK210922. Our gratitude goes to Juan Contreras, Isabela Macias and Juan Manuel Wagner for their contributions to seismic and illustration software management. We are grateful to UABC and CONAHCYT for the founding of this project. This work is contribution No. 8 from the academic team *Geología Costera UABC-CA-38*.

Financing

This work has been founded by CONAHCYT [grant number 1011828, 319430]; UABC [grant number 401/1/C/13/23].

References

Atwater, T. (1970). Implications of plate tectonics for the Cenozoic tectonic evolution of western North America. Geological Society of America Bulletin, 81(12), 3513-3536. https://doi.org/10.1130/0016-7606(1970)81[3513:IOPTFT]2.0.CO;2

Atwater, T. and Stock, J. (1998). Pacific-North America plate tectonics of the Neogene southwestern United States: an update. International Geology Review, 40(5), 375-402. https://doi.org/10.1080/00206819809465216

Balestrieri, M.L., Ferrari, L., Bonini, M., Duque-Trujillo, J., Cerca, M., Moratti, G., & Corti, G. (2017). Onshore and offshore apatite fission-track dating from the southern Gulf of California: Insights into the time-space evolution of the rifting: Tectonophysics, 719, 148-161. https://doi.org/10.1016/j.tecto.2017.05.012

Bennett, S. E., Oskin, M. E., Iriondo, A., & Kunk, M. J. (2016). Slip history of the La Cruz fault: Development of a late Miocene transform in response to increased rift obliquity in the northern Gulf of California. Tectonophysics, 693, 409-435. https://doi.org/10.1016/j.tecto.2016.06.013

ISSN-On line: 2444-4987

Bohannon, R. G., & Parsons, T. (1995). Tectonic implications of post–30 Ma Pacific and North American relative plate motions. Geological Society of America Bulletin, 107(8), 937-959. https://doi.org/10.1130/0016-7606(1995)107<0937:TIOPMP>2.3.CO;2

Bot, A., Geoffroy, L., Authemayou, C., Bellon, H., Graindorge, D., & Pik, R. (2016). Miocene detachment faulting predating EPR propagation: Southern Baja California. Tectonics, 35(5), 1153-1176. https://doi.org/10.1002/2015TC004030

Buck, W. R. (1988). Flexural rotation of normal faults. Tectonics, 7(5), 959-973. https://doi.org/10.1029/TC007i005p00959

Buck, W. R. (1993). Effect of lithospheric thickness on the formation of high-and low-angle normal faults. Geology, 21(10), 933-936. https://doi.org/10.1130/0091-7613(1993)021<0933:EOLTOT>2.3.CO;2

Bunge, H. P., & Grand, S. P. (2000). Mesozoic plate-motion history below the northeast Pacific Ocean from seismic images of the subducted Farallon slab. Nature, 405(6784), 337-340. 10.1038/35012586

Canales, J. P., Detrick, R. S., Lin, J., Collins, J. A., & Toomey, D. R. (2000). Crustal and upper mantle seismic structure beneath the rift mountains and across a nontransform offset at the Mid Atlantic Ridge (35 N). Journal of Geophysical Research: Solid Earth, 105(B2), 2699-2719. https://doi.org/10.1029/1999JB900379

Canales, J.P, Detrick, R. S., Toomey, D. R., & Wilcock, W. S. (2003). Segment-scale variations in the crustal structure of 150–300 kyr old fast spreading oceanic crust (East Pacific Rise, 8 15′ N–10 5′ N) from wide-angle seismic refraction profiles. Geophysical Journal International, 152(3), 766-794. https://doi.org/10.1046/j.1365-246X.2003.01885.x

Chopra, S., Marfurt, K.J. (2007), Seismic attributes for prospect identification and reservoir characterization. Tulsa, Oklahoma, U.S.A., Society of Exploration Geophysicists and European Association of Geoscientists and Engineers, 457 pp. https://doi.org/10.1190/1.9781560801900

Di Luccio, F., Persaud, P., Clayton, R.W. (2014). Seismic structure beneath the Gulf of California: a contribution from group velocity measurements. Geophys. J. Int. 199, 1861–1877. https://doi.org/10.1093/gji/ggu338

Dooley, T.P., & McClay, K. (1997). Analog modeling of pull-apart basins. AAPG (Am. Assoc. Pet. Geol.) Bull. 81 (11), 1804–1826. https://doi.org/10.1306/3B05C636-172A-11D7-8645000102C1865D

Escartín, J., & Lin, J. (1995). Ridge offsets, normal faulting, and gravity anomalies of slow spreading ridges. Journal of Geophysical Research: Solid Earth, 100(B4), 6163-6177. https://doi.org/10.1029/94JB03267

Ferrari, L., Orozco-Esquivel, T., Bryan, S. E., Lopez-Martinez, M., & Silva-Fragoso, A. (2018). Cenozoic magmatism and extension in western Mexico: Linking the Sierra Madre Occidental silicic large igneous province and the Comondú Group with the Gulf of California rift. Earth-Science Reviews, 183, 115-152. https://doi.org/10.1016/j.earscirev.2017.04.006

Fletcher, J. M., & Munguia, L. (2000). Active continental rifting in southern Baja California, Mexico: Implications for plate motion partitioning and the transition to seafloor spreading in the Gulf of California. Tectonics, 19(6), 1107-1123. https://doi.org/10.1029/1999TC001131

Fletcher, J. M., Kohn, B. P., Foster, D. A., & Gleadow, A. J. (2000). Heterogeneous Neogene cooling and exhumation of the Los Cabos block, southern Baja California: Evidence from fission-track thermochronology. Geology, 28(2), 107-110. https://doi.org/10.1130/0091-7613(2000)28<107:HNCAEO>2.0.CO;2

Fletcher, J. M., Grove, M., Kimbrough, D., Lovera, O., & Gehrels, G. E. (2007). Ridge-trench interactions and the Neogene tectonic evolution of the Magdalena shelf and southern Gulf of California: Insights from detrital zircon U-Pb ages from the Magdalena fan and adjacent areas. Geological Society of America Bulletin, 119(11-12), 1313-1336. https://doi.org/10.1130/B26067.1

ISSN-On line: 2444-4987

Fletcher, J. M., & Spelz, R. M. (2009). Patterns of Quaternary deformation and rupture propagation associated with an active low-angle normal fault, Laguna Salada, Mexico: Evidence of a rolling hinge? Geosphere, 5(4), 385-407. https://doi.org/10.1130/GES00206.1

Gerya, T. (2010). Dynamical instability produces transform faults at mid-ocean ridges. Science, 329(5995), 1047-1050. 10.1126/science.11913

Gregg, P. M., Lin, J., & Smith, D. K. (2006). Segmentation of transform systems on the East Pacific Rise: Implications for earthquake processes at fast-slipping oceanic transform faults. Geology, 34(4), 289-292. https://doi.org/10.1130/G22212.1

Gregg, P. M., Lin, J., Behn, M. D., & Montési, L. G. (2007). Spreading rate dependence of gravity anomalies along oceanic transform faults. Nature, 448(7150), 183-187. 10.1038/nature05962

Howell, S. M., Olive, J. A., Ito, G., Behn, M. D., Escartin, J., & Kaus, B. (2019). Seafloor expression of oceanic detachment faulting reflects gradients in mid-ocean ridge magma supply. Earth and Planetary Science Letters, 516, 176-189. https://doi.org/10.1016/j.epsl.2019.04.001

Julià-Miralles, M., Yarbuh, I., Spelz, R.M., Negrete-Aranda, R., Contreras, J., Fletcher, J.M., González-Fernández, A., Zierenberg, R., Caress, D.W. (submmited). Crustal structure and tectonic history of the Carmen Basin, southern Gulf of California: insights from high-resolution bathymetry and 2D seismic reflection profiles. Marine and Petroleum Geology. Available at SSRN: https://ssrn.com/abstract=4303241 or http://dx.doi.org/10.2139/ssrn.4303241

Kluesner, J.W., 2011. Marine geophysical study of cyclic sedimentation and shallow sill intrusion in the floor of the Central Gulf of California. UC San Diego (Ph.D. Thesis, 231 pp). https://escholarship.org/content/qt28r533bv/qt28r533bv.pdf

Kuo, B. Y., & Forsyth, D. W. (1988). Gravity anomalies of the ridge-transform system in the South Atlantic between 31 and 34.5 S: Upwelling centers and variations in crustal thickness. Marine Geophysical Researches, 10(3), 205-232. https://doi.org/10.1007/BF00310065

Lavier, L. L., Roger Buck, W., & Poliakov, A. N. (1999). Self-consistent rolling-hinge model for the evolution of large-offset low-angle normal faults. Geology, 27(12), 1127-1130. https://doi.org/10.1130/0091-7613(1999)027<1127:SCRHMF>2.3.CO;2

Lin, J., Purdy, G. M., Schouten, H., Sempere, J. C., & Zervas, C. (1990). Evidence from gravity data for focusedmagmatic accretionalong the Mid-Atlantic Ridge. Nature, 344(6267), 627-632. https://doi.org/10.1038/344627a0

Lizarralde, D., Axen, G. J., Brown, H. E., Fletcher, J. M., González-Fernández, A., Harding, A. J., ... & Umhoefer, P. J. (2007). Variation in styles of rifting in the Gulf of California. Nature, 448(7152), 466-469. https://doi.org/10.1038/nature06035

Macias-Iñiguez, I., Yarbuh, I., Spelz-Madero, R., González-Fernández, A., Fletcher, J. M., Contreras, J., ... & Guardado-France, R. (2019). Modo de extensión de la corteza y formación del Sistema Extensional de Cerralvo, sur del Golfo de California, a partir de datos de reflexión sísmica en 2D. Revista Mexicana de Ciencias Geológicas, 36(3), 334-347. https://doi.org/10.22201/cgeo.20072902e.2019.3.1352

Martín-Barajas, A., González-Escobar, M., Fletcher, J. M., Pacheco, M., Oskin, M., & Dorsey, R. (2013). Thick deltaic sedimentation and detachment faulting delay the onset of continental rupture in the Northern Gulf of California: Analysis of seismic reflection profiles. Tectonics, 32(5), 1294-1311. https://doi.org/10.1002/tect.20063

Negrete-Aranda, R., Contreras, J., & Spelz, R. M. (2013). Viscous dissipation, slab melting, and post-subduction volcanism in south-central Baja California, Mexico. Geosphere, 9(6), 1714-1728. https://doi.org/10.1130/GES00901.1

Negrete-Aranda, R., Neumann, F., Harris, R. N., Contreras, J., Zierenberg, R. A., & Caress, D. W. (2019). First Heat Flow Measurements in the Auka and JaichMaa'ja'ag vent fields Pescadero Basin, Southern Gulf of California. In AGU Fall Meeting Abstracts (Vol. 2019, pp. V13D-0187). Available at https://ui.adsabs.harvard.edu/abs/2019AGUFM.V13D0187N/abstract

Negrete-Aranda, R., Neumann, F., Contreras, J., Harris, R.N., Spelz, R.M., Zierenberg, R., Caress, D.W. (2021). Transport of Heat by Hydrothermal Circulation in a Young Rift Setting: Observations from the Auka and JaichMaa ja' ag' vent Fields in the Pescadero Basin, Southern Gulf of California. Journal of Geophysical Research: Solid Earth. https://doi.org/10.1029/2021JB022300

Nicholson, C., Sorlien, C. C., Atwater, T., Crowell, J. C., & Luyendyk, B. P. (1994). Microplate capture, rotation of the western Transverse Ranges, and initiation of the San Andreas transform as a low-angle fault system. Geology, 22(6), 491-495. https://doi.org/10.1130/0091-7613(1994)022<0491:MCROTW>2.3.CO;2

Piñero-Lajas, D. (2008). Seismic reflection and 40Ar-39Ar dating of continental basement in the western margin of Farallon basin (southern Gulf of California, Mexico). CICESE, Ensenada, Baja California, México (M.Sc. thesis in Earth Science. 155 pp). https://cicese.repositorioinstitucional.mx/jspui/handle/1007/2628. Available at https://biblioteca.cicese.mx/catalogo/tesis/ficha.php?id=17932

Ramírez-Zerpa, N., Spelz, R. M., Yarbuh, I., Negrete-Aranda, R., Contreras, J., Clague, D. A., ... & González-Fernández, A. (2022). Architecture and tectonostratigraphic evolution of the Pescadero Basin Complex, southern Gulf of California: Analysis of high-resolution bathymetry data and seismic reflection profiles. Journal of South American Earth Sciences, 103678. https://doi.org/10.1016/j.jsames.2021.103678

Sarkar, S., Moser, M., Berndt, C., Doll, M., Böttner, C., Chi, W. C., ... & Hensen, C. (2022). Thermal state of the Guaymas Basin derived from gas hydrate bottom simulating reflections and heat flow measurements. Journal of Geophysical Research: Solid Earth, 127(8), e2021JB023909. https://doi.org/10.1029/2021JB023909

Spencer, J. E., & Normark, W. R. (1979). Tosco-Abreojos fault zone: A Neogene transform plate boundary within the Pacific margin of southern Baja California, Mexico. Geology, 7(11), 554-557. https://doi.org/10.1130/0091-7613(1979)7<554:TFZANT>2.0.CO;2

Stock, J. M., & Hodges, K. V. (1989). Pre-Pliocene extension around the Gulf of California and the transfer of Baja California to the Pacific plate. Tectonics, 8(1), 99-115. https://doi.org/10.1029/TC008i001p00099

Sutherland, F.H., Kent, G.M., Harding, A.J., Umhoefer, P.J., Driscoll, N.W., Lizarralde, D., Fletcher, J.M., Axen, J.G., Holbrook, W.S., González-Fernández, A., Lonsdale, P. (2012). Middle Miocene to early Pliocene oblique extension in the southern Gulf of California. Geosphere 8 (4), 752–770. https://doi.org/10.1130/GES00770.1

Umhoefer, P. J. (2011). Why did the Southern Gulf of California rupture so rapidly?—Oblique divergence across hot, weak lithosphere along a tectonically active margin. GSA Today, 21(11), 4-10. https://doi.org/10.1130/G133A.1.

Umhoefer, P. J., Darin, M. H., Bennett, S. E., Skinner, L. A., Dorsey, R. J., & Oskin, M. E. (2018). Breaching of strike-slip faults and successive flooding of pull-apart basins to form the Gulf of California seaway from ca. 8–6 Ma. Geology, 46(8), 695-698. 10.1130/G40242.1

Umhoefer, P.J., Plattner, C., and Malservisi, R. (2020). Quantifying rates of "rifting while drifting" in the southern Gulf of California: The role of the southern Baja California microplate and its eastern boundary zone: Lithosphere, v. 12, p. 122–132. https://doi.org/10.1130/L1132.1

Wang, Y., Forsyth, D. W., & Savage, B. (2009). Convective upwelling in the mantle beneath the Gulf of California. Nature, 462(7272), 499-501. 10.1038/nature08552

ISSN-On line: 2444-4987

Wang, Y., Forsyth, D. W., Rau, C. J., Carriero, N., Schmandt, B., Gaherty, J. B., & Savage, B. (2013). Fossil slabs attached to unsubducted fragments of the Farallon plate. Proceedings of the National Academy of Sciences, 110(14), 5342-5346. https://doi.org/10.1073/pnas.1214880110

Wernicke, B., & Axen, G. J. (1988). On the role of isostasy in the evolution of normal fault systems. Geology, 16(9), 848-851. https://doi.org/10.1130/0091-7613(1988)016<0848:OTROII>2.3.CO;2

Wright, N. M., Seton, M., Williams, S. E., & Mueller, R. D. (2016). The Late Cretaceous to recent tectonic history of the Pacific Ocean basin. Earth-Science Reviews, 154, 138-173. https://doi.org/10.1016/j.earscirev.2015.11.015

Wu, J.E., McClay, K., Whitehouse, P., and Dooley, T. (2009), 4D analogue modelling of transtensional pull-apart basins: Marine and Petroleum Geology, v. 26, p. 1608–1623. https://doi.org/10.1016/j.marpetgeo.2008.06.007

Yilmaz, Ö. (2001). Seismic data analysis: Processing, inversion, and interpretation of seismic data, vol. 1, Society of Exploration Geophysicists, Tulsa, 2027 pp. https://doi.org/10.1190/1.9781560801580.fm

Zhao, D. (2004). Global tomographic images of mantle plumes and subducting slabs: insight into deep Earth dynamics. Physics of the Earth and Planetary Interiors, 146(1-2), 3-34. https://doi.org/10.1016/j.pepi.2003.07.032

ISSN-On line: 2444-4987